Influence of Mn-doping concentration on the microstructure and magnetic properties of ZnO thin films*

WU Zhao-feng (吴兆丰)[1]**, **GUO Lei** (郭磊)[1], **CHENG Kun** (程鲲)[1], **ZHANG Feng** (张峰)[2], and **GUAN Rong-feng** (关荣锋)[3]

1. School of Mathematics and Physics, Yancheng Institute of Technology, Yancheng 224051, China

2. Civil Engineering Department, Yancheng Institute of Technology, Yancheng 224051, China

3. Key Laboratory for Advanced Technology in Environmental Protection of Jiangsu Province, Yancheng Institute of Technology, Yancheng 224051, China

(Received 25 November 2015)

The microstructure and magnetic properties of Mn-doped ZnO films with various Mn contents, synthesized by magnetron sputtering at room temperature, are investigated in detail. X-ray diffraction (XRD) measurement results suggest that the doped Mn ions occupy the Zn sites successfully and do not change the crystal structure of the ZnO films. However, the microstructure of the Mn-doped ZnO films apparently changes with increasing the Mn concentration. Arrays of well-aligned nanoscale rods are found in the Mn-doped ZnO films with moderate Mn concentrations. Magnetic measurement results indicate that the ZnO films doped with moderate Mn concentration are ferromagnetic at room temperature. The possible origin of the ferromagnetism in our samples is also explored in detail.

Document code: A **Article ID:** 1673-1905(2016)01-0052-4

DOI 10.1007/s11801-016-5236-x

Diluted magnetic semiconductors (DMS) have attracted considerable attention in recent years because of their rich potential applications in spintronics[1,2]. Much focus of DMS research is to dope transitional metals into various semiconductor materials. Among the semiconductor candidates, the ZnO doped with 3d transitional metals (TMs) has gained significant attention because the resultant materials can be used as DMS with a Curie temperature above room temperature (RT)[1,3-5]. A drawback to this approach is that the dopant materials can segregate to form precipitates or clusters that are responsible for ferromagnetic properties. The effect of such ferromagnetic clusters must be examined more carefully before such materials can be applied in spintronics applications[4].

Mn is a promising doping element to distinguish intrinsic ferromagnetism from the secondary phases or precipitates in DMS[5,6]. Following the theoretical predictions[4] of ferromagnetism in Mn-doped bulk ZnO, considerable experimental effort has been devoted to this system. However, the experimental results are in conflict with each other, and the reproducibility of ferromagnetic behavior is still a challenging problem[7]. Several groups have obtained different properties in Mn-doped ZnO, such as spin-glass behavior[8], paramagnetism[9] and ferromagnetism[10]. These magnetic properties are strongly dependent on the sample preparation conditions. Hence, there are many reports on the growth of Mn-doped ZnO thin films by different techniques[7]. In this paper, $Zn_{1-x}Mn_xO$ films with x=0, 0.017, 0.029, 0.044 and 0.067 were fabricated by the magnetron sputtering technique. The effects of Mn doping on the microstructure and magnetic properties and their interplays in ZnO films are discussed in detail.

The Mn-doped ZnO films were grown on Si and quartz glass substrates by magnetron sputtering using a composite target of a ZnO (60 mm in diameter) ceramic containing several Mn pieces on the surface. The number of Mn pieces could be changed to adjust the concentration of Mn in the films. The deposition chamber was evacuated by a molecular pump to a base pressure below 6×10^{-4} Pa. Pure argon gas was introduced into the chamber as the working gas using a mass flow controller. The flow rate was regulated at 20 cm^3/min, and the chamber pressure was fixed at 2.0 Pa. Prior to deposition, pre-sputtering cleaning was performed for 10 min to remove possible contaminants from the target. Deposition was then conducted at a radio frequency (RF) power of 100 W and at RT.

The thickness of the films was approximately 320 nm, which was measured by a surface profilometer (Kosaka ET-350). The structural qualities of the samples were investigated by X-ray diffraction (XRD) (Rigaku D/max-3C) using Cu Kα radiation. The magnified cross-sectional morphology was examined by field-emission

* This work has been supported by the National Natural Science Foundation of China (Nos.11204266 and 21276220), and the Nature Science Foundation of Jiangsu Province (No.BK20141262).

** E-mail: wuzhaofeng@126.com

scanning electron microscopy (FE-SEM) using a Hitachi S-4700 instrument. The Mn concentration in the samples was evaluated by energy-dispersive X-ray spectroscopy (Hitachi S-4700) analysis. X-ray photoelectron spectroscopy (XPS) was performed by using an X-ray photoemission spectrometer (KRATOS Analytical). Magnetic measurements were performed using a quantum-design superconducting quantum interference device (SQUID) magnetometer with the magnetic field parallel to the film surface. Electrical resistivity measurements were made using the four-point probe system with current of 1 mA.

Fig.1 shows the XRD patterns for the $Zn_{1-x}Mn_xO$ films with x=0, 0.017, 0.029, 0.044 and 0.067. All films exhibit a nearly single-phase wurtzite structure with the *c*-axis normal to the Si substrate surface[11,12]. No peak corresponding to Mn/Mn oxide or any other secondary phases is discerned in the XRD patterns for any Mn-doped ZnO samples. This indicates that, within the XRD detection limits, all the Mn-doped ZnO films are monophasic. The *c*-axis lattice constants, the full width at half-maximum (*FWHM*) of the (002) diffraction peak and the mean grain size (*D*) perpendicular to the reflecting plane in the film as estimated by Scherrer's formula are summarized in Tab.1. The slight increase of the *c*-axis lattice constants with increase of Mn doping concentration may be due to the incorporation of Mn into the ZnO lattice. Whit the increase of Mn doping concentration, the calculated mean grain size shows an increasing trend at low Mn concentrations but deviates at higher concentrations, which indicates that the ZnO grain growth along the *c*-axis can be reinforced by moderate Mn doping.

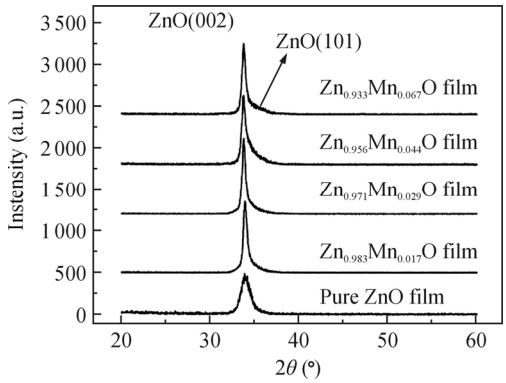

Fig.1 XRD patterns for $Zn_{1-x}Mn_xO$ films

Fig.2 shows FE-SEM images for the cross-sections of the $Zn_{1-x}Mn_xO$ film deposited on Si substrates. Aligned nanoscale rod arrays perpendicular to the substrates are found in the SEM micrographs for the $Zn_{0.983}Mn_{0.017}O$, $Zn_{0.971}Mn_{0.029}O$ and $Zn_{0.956}Mn_{0.044}O$ films. The diameter of each nanorod has little variation from bottom to top, with the average diameter being 20—30 nm, as shown in the insets of Fig.2(b)—(d). In contrast, rare nanorods can be detected in pure ZnO and $Zn_{0.933}Mn_{0.067}O$ films. These images indicate that Mn doping at a moderate concentration may promote the growth of aligned nanoscale columnar grains along the *c*-axis, but the growth may be degraded at a higher Mn concentration, as expected from the XRD result. Hence, we suggest that the method in our experiments may be applied to the large-scale manufacture of aligned Mn-doped ZnO nanorod arrays with moderate Mn concentration.

Tab.1 The *c*-axis lattice constants, the *FWHM* of (002) diffraction peak and the mean grain size (*D*) along the *c*-axis of the $Zn_{1-x}Mn_xO$ films

Sample	*c* (nm)	*FWHM* (°)	*D* (nm)
Pure ZnO film	0.527 8±0.000 2	0.872	11.0±0.4
$Zn_{0.983}Mn_{0.017}O$ film	0.528 4±0.000 2	0.463	20.7±1.0
$Zn_{0.971}Mn_{0.029}O$ film	0.530 6±0.000 2	0.502	19.0±0.8
$Zn_{0.956}Mn_{0.044}O$ film	0.530 9±0.000 2	0.515	18.6±0.8
$Zn_{0.933}Mn_{0.067}O$ film	0.530 9±0.000 2	0.513	18.6±0.8

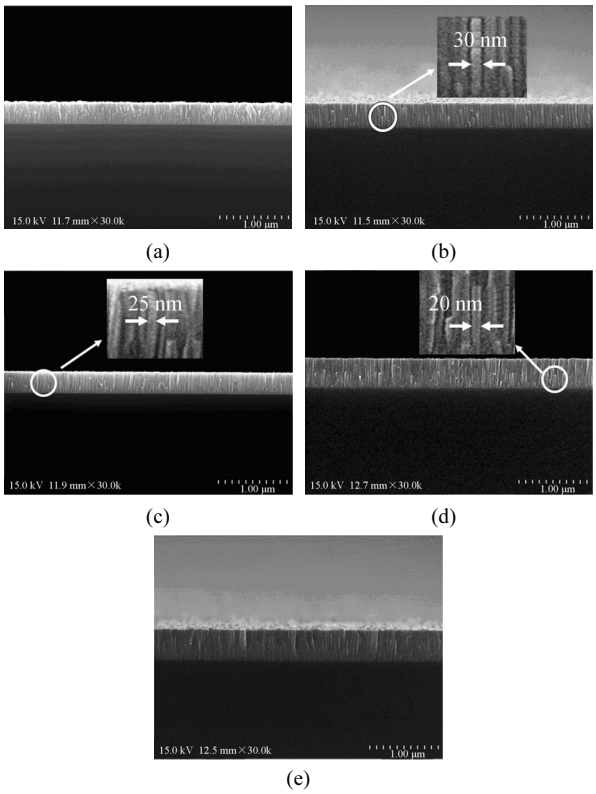

Fig.2 Cross-sectional SEM images of (a) pure ZnO, (b) $Zn_{0.983}Mn_{0.017}O$, (c) $Zn_{0.971}Mn_{0.029}O$, (d) $Zn_{0.956}Mn_{0.044}O$ and (e) $Zn_{0.933}Mn_{0.067}O$ films

To obtain more information related to the magnetic properties of the samples, XPS measurements were made to identify the binding state of the cations in the samples. The fine-scanned XPS spectra of the $Zn_{1-x}Mn_xO$ films were recorded after Ar ion sputtering for 2 min to remove the adsorbed contaminants on surface, as shown in Fig.3. It is observed in Fig.3(a) that as the Mn concentration increases from x=0.017 to x=0.067, the Mn $2p_{3/2}$ peak of

the films remains at 640.8 eV, which is clearly different from those of Mn metal at 638.8 eV and Mn^{4+} at 642.2 eV. The peak at 640.8 eV can be indexed to the Mn^{2+} ion, as it matches well with the reported binding energy of the Mn^{2+} state[13]. Therefore, it can be concluded that the Mn element in the films exists mainly in the form of Mn^{2+}. Fig.3(b) corresponds to the fine-scanned Zn $2p_{3/2}$ peak of the $Zn_{1-x}Mn_xO$ films. We can see from Fig.3(b) that the core level binding energy for the Zn $2p_{3/2}$ primary peak is at 1 022.1 eV, which remains unchanged with the increase of Mn concentration. The narrow widths of these peaks indicate that Zn^{2+} ions are dominant in these samples. Mn^{2+}, with a large ionic radius, replacing the lattice Zn^{2+} of ZnO can result in the increasing binding energy of Zn^{2+}. As a result, the peak centered at 1 022.1 eV is slightly larger than that of Zn^{2+} in the bulk ZnO (1 021.4 eV). In addition, these results indicate that there is no $ZnMn_2O_4$ formed in the films. In $ZnMn_2O_4$, the Mn^{3+} ionic radius (0.066 nm) is smaller than that of Zn^{2+} (0.074 nm), which results in the binding energy of Zn shifting to the low-energy side[14]. So if there is any $ZnMn_2O_4$ in the films, the Zn $2p_{3/2}$ spectrum for the samples should exhibit an asymmetry feature and involve a peak component centered at the binding energy smaller than that of Zn^{2+} in the bulk ZnO (1 021.4 eV). However, Zn $2p_{3/2}$ peaks for our samples are all centered at 1 022.1 eV and very symmetric. Thus, we suggest that there is no $ZnMn_2O_4$ formed in our samples.

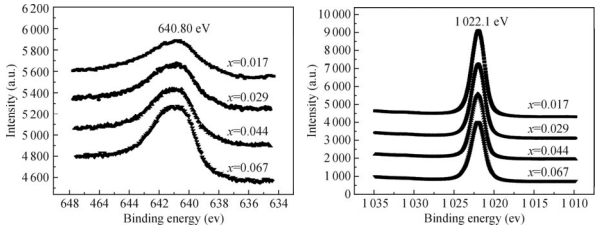

Fig.3 Fine-scanned XPS spectra of (a) Mn $2p_{3/2}$ and (b) Zn $2p_{3/2}$ in the $Zn_{1-x}Mn_xO$ films

Magnetic measurements on $Zn_{1-x}Mn_xO$ films were performed using an SQUID magnetometer. All the measurements were corrected for substrate effects. Magnetization loops (magnetization per atom versus magnetic field strength H) for $Zn_{1-x}Mn_xO$ films measured at 300 K are shown in Fig.4. It can be seen that $Zn_{0.983}Mn_{0.017}O$ film is in a paramagnetic state, while the other $Zn_{1-x}Mn_xO$ films with x=0.029, 0.044 and 0.067 exhibit hysteresis loops, indicating the ferromagnetism at room temperature. The 2.9% Mn-doped sample possesses the largest saturated magnetization per atom (M_S) of 3.2×10^{-24} A·m^2 per Mn atom, the 4.4% Mn-doped sample has an M_S of 1.8×10^{-24} A·m^2 per Mn atom, and the 6.7% Mn-doped sample has an M_S of 1.5×10^{-24} A·m^2 per Mn atom. The M_S of the 2.9% Mn-doped sample is comparable with the values found in earlier reports, namely 1.4×10^{-24}—1.6×10^{-24} A·m^2 per Mn atom in thin films[10], 1.5×10^{-24} A·m^2 per Mn atom in bulk materials[15] and 8.5×10^{-24} A·m^2 per Mn atom in (N, Mn)-codoped ZnO thin films[16]. However, these data are much smaller than ~4.6×10^{-23} A·m^2 per Mn atom for a free Mn^{2+} ion with S=5/2 and g=2. It is suggested that there is a competition between antiferromagnetic and ferromagnetic interactions. Because of the competition, the M_S of the Mn ion in the films is much smaller than the theoretical value for the free Mn^{2+} ion.

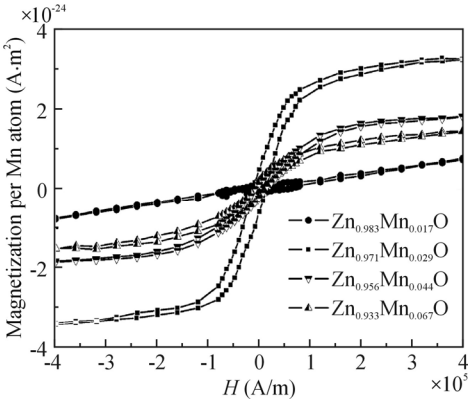

Fig.4 Magnetization per Mn atom versus H for $Zn_{1-x}Mn_xO$ films at RT

Now, we discuss the origin of ferromagnetism in $Zn_{1-x}Mn_xO$ films. Let us consider the possibility of the formation of Mn-related secondary phases. The secondary phases are a kind of concern in any diluted magnetic system as a source of spurious magnetic signals. Among the impurity phases related to a Mn:ZnO system, $ZnMn_2O_4$ is the only ferromagnetic phase at RT. However, neither $ZnMn_2O_4$ nor other secondary phases were detected via XRD and XPS. The stronger ferromagnetic behavior in samples with a lower Mn concentration of 2.9%, as well as its apparent weakening at higher doping concentrations, also confirms the absence of Mn-related ferromagnetic precipitates. If the formation of a secondary Mn-related phase is responsible for the RT ferromagnetic behavior, an increase in Mn concentration would presumably increase the secondary phase volume fraction and related magnetization signature. Instead, the opposite behavior is observed. As discussed above, the observed RT ferromagnetism is not from the Mn-related secondary phases. The most probable reason for the magnetic properties is ferromagnetic coupling of Mn atoms dissolved in the ZnO matrix.

To date, the origin of ferromagnetism in DMS materials has been a very controversial topic. In order to address the origin of ferromagnetism in $Zn_{1-x}Mn_xO$ films, the electrical resistance of the samples was measured. The resistivity of the films is of the order of 10^4 Ω·cm. This seems to contradict a free-carrier-mediated mechanism (such as the Ruderman-Kittel-Kasuya-Yosida model) for ferromagnetism in $Zn_{1-x}Mn_xO$ films. Moreover, conventional superexchange interactions cannot produce long-range

magnetic order when the concentrations of magnetic cations are only a few percent, i.e., Mn-doped ZnO with Mn doping atom percent of 2.9%. Recently, Zou's research[17] indicated that the defects may play an important role in the origin of RT ferromagnetism in Mn:ZnO. According to our previous research[18], considerable point defects, such as oxygen vacancies (V_O), are considered to exist in the Mn-doped ZnO films. Kittilstved et al[19] had suggested one kind of mechanism for magnetic ordering in DMS, which is called bound magnetic polarons model. In this model, the electrons associated with shallow donor defects in the samples (here V_O) are energetically aligned with the $TM^{+/2+}$ level (here Mn^{2+}), leading to effective dopant-defect hybridization, which can lead to an effective ferromagnetic coupling between dopant Mn atoms. The radius of this trapped electron orbital is estimated to be of the order of $a_0\varepsilon$, where a_0 is the Bohr radius, and ε is the dielectric constant of the samples. For ZnO, this value is on the order of 0.5 nm, which is enough to contain a dopant atom in the 2.9% Mn-doped ZnO film but is not enough in the 1.7% Mn-doped sample. Therefore, the $Zn_{1-x}Mn_xO$ films with x=0.029, 0.044 and 0.067 exhibit ferromagnetic properties, while the $Zn_{0.983}Mn_{0.017}O$ film is in a paramagnetic state. On the other hand, for $Zn_{1-x}Mn_xO$ films with high Mn content (x>2.9%), an increase of the dopant concentration is found to cause a decrease of M_S owing to an increased number of Mn atoms occupying adjacent cation lattice positions that results in an antiferromagnetic alignment. As a consequence, the maximum value of M_S is 3.2×10^{-24} A·m^2 per Mn atom, at the lower Mn concentration of 2.9%, under our experimental conditions.

In summary, RT ferromagnetism was observed in $Zn_{1-x}Mn_xO$ films with $0.029\leq x\leq0.067$ prepared by the magnetron sputtering method. Structural characterization using XRD and XPS was done to provide evidence for the absence of any secondary ferromagnetic phase in $Zn_{1-x}Mn_xO$ films with $x\leq0.067$. Nanoscale Mn-doped ZnO rod arrays were found in the FE-SEM images. There is a narrow processing window in terms of doping concentration at which effective ferromagnetic doping of ZnO is possible, which also avoids the secondary phase formation and maintains the growth of nanoscale rod arrays. The ferromagnetism in the films can be described by bound magnetic polarons models with respect to defect-bound carriers. As the magnetron sputtering method can produce economically feasible large-area films with well-controlled composition, we suggest that our method may be applied to future large-scale manufacture of aligned Mn-doped ZnO nanorod arrays with RT ferromagnetism.

References

[1] T. Dietl, H. Ohno, F. Matsukura, J. Cibert and D. Ferrand, Science **287**, 1019 (2000).

[2] H. Y. Man, S. L. Guo, Y. Sui, Y. Guo, B. Chen, H. D. Wang, C. Ding and F. L. Ning, Scientific Reports **5**, 15507 (2015).

[3] J. M. D. Coey, P. Stamenov, R. D. Gunning, M. Venkatesan and K. Paul, New Journal of Physics **12**, 053025 (2010).

[4] S. J. Pearton, W. H. Heo, M. Ivill, D. P. Norton and T. Steiner, Semiconductor Science and Technology **19**, R59 (2004).

[5] M. Chakrabarti, S. Dechoudhury, D. Sanyal, T. K. Roy, D. Bhowmick and A. Chakrabarti, Journal of Physics D: Applied Physics **41**, 135006 (2008).

[6] Z. L. Lu, G. Q. Yan, S. Wang, W. Q. Zou, Z. R. Mo, L. Y. Lv, F. M. Zhang, Y. W. Du, M. X. Xu and Z. H. Xia, Journal of Applied Physics **104**, 033919 (2008).

[7] J. Elanchezhiyan, K. P. Bhuvana, N. Gopalakrishnan and Y. Balasubramanian, Materials Letters **62**, 3379 (2008).

[8] T. Fukumura, Z. Jin, M. Kawasaki, T. Shono, T. Hasegawa, S. Koshihara and H. Koinuma, Applied Physics Letters **78**, 958 (2001).

[9] A. Tiwari, C. Jin, A. Kvit, D. Kumar, J. F. Muth and J. Nrayan, Solid State Communications **121**, 371 (2002).

[10] S. W. Jung, S. T. An, G. Yi, U. Jung, S. Lee and S. Cho, Applied Physics Letters **80**, 4561 (2002).

[11] ZI Xing-fa, YE Qing, LIU Rui-ming and HE Yong-tai, Journal of Optoelectronics·Laser **26**, 883 (2015). (in Chinese)

[12] ZHANG Zhong-jun, ZHANG Li-chun, ZHAO Feng-zhou, QU Chong, HUANG Rui-zhi, ZHANG Min and Li Qing-shan, Journal of Optoelectronics·Laser **25**, 851 (2014). (in Chinese)

[13] L. W. Yang, X. L. Wu, G. S. Huang, T. Qiu and Y. M. Yang, Journal of Applied Physics **97**, 014308 (2005).

[14] J. H. Li, D. Z. Shen, J. Y. Zhang, D. X. Zhao, B. S. Li, Y. M. Lu, Y. C. Liu and X. W. Fan, Journal of Magnetism and Magnetic Materials **302**, 118 (2006).

[15] X. M. Cheng and C. L. Chien, Journal of Applied Physics **93**, 7876 (2003).

[16] Z. B. Gu, M. H. Liu, J. Wang, D. Wu, S. T. Zhang, X. K. Meng, Y. Y. Zhu, S. N. Zhu, Y. F. Chen and X. Q. Pan, Applied Physics Letters **88**, 082111 (2006).

[17] C. W. Zou, H. J. Wang, M. L. Yi, M. Li, C. S. Liu, L. P. Guo, D. J. Fu, T. W. Kang, Applied Surface Science **256**, 2453 (2010).

[18] Z. F. Wu, X. M. Wu, L. J. Zhuge, X. M. Chen and X. F. Wang, Applied Physics Letters **93**, 023103 (2008).

[19] K. R. Kittilstved, W. K.Liu and D. R. Gamelin, Nature Materials **5**, 291 (2006).